Substrate Recognition and Catalysis by the Cofactor-Independent Dioxygenase DpgC[†,‡]

Elisha N. Fielding, Paul F. Widboom, and Steven D. Bruner*

Department of Chemistry, Merkert Chemistry Center, Boston College, Chestnut Hill, Massachusetts 02467

Received June 11, 2007; Revised Manuscript Received October 7, 2007

ABSTRACT: The enzyme DpgC belongs to a small class of oxygenases not dependent on accessory cofactors for activity. DpgC is in the biosynthetic pathway for the nonproteinogenic amino acid 3,5-dihydroxyphenylglycine in actinomycetes bacteria responsible for the production of the vancomycin/teicoplanin family of antibiotic natural products. The X-ray structure of DpgC [Widboom, P. W., Fielding, E. N., Liu, Y., and Bruner, S. D. (2007) *Nature 447*, 342−345] confirmed the absence of cofactors and defined a novel hydrophobic dioxygen binding pocket adjacent to a bound substrate analogue. In this paper, the role specific amino acids play in substrate recognition and catalysis is examined through biochemical and structural characterization of site-specific enzyme mutations and alternate substrates. The results establish the importance of three amino acids, Arg254, Glu299, and Glu189, in the chemistry of DpgC. Arg254 and Glu189 join to form a specific contact with one of the phenolic hydroxyls of the substrate, and this interaction plays a key role in both substrate recognition and catalysis. The X-ray crystal structure of Arg254Lys was determined to address the role this residue plays in the chemistry. In addition, characterization of alternate substrate analogues demonstrates the presence and position of phenol groups are necessary for both enzyme recognition and downstream oxidation chemistry. Overall, this work defines the mechanism of substrate recognition and specificity by the cofactor-independent dioxygenase DpgC.

The cofactor-independent dioxygenase DpgC catalyzes a key reaction in the biosynthesis of the nonproteinogenic amino acid 3,5-dihydroxyphenylglycine (DPG,[1] **5**) (*1*, *2*). DPG is incorporated into the vancomycin (**1**) and teicoplanin (**2**) family of antibiotics by a nonribosomal peptide synthetase (NRPS) pathway (*3*), participating in biaryl cross-links in the peptide natural products (Figure 1A). This structural motif contributes to a rigid framework allowing the antibiotics to bind the cell wall biosynthesis precursor D-Ala−D-Ala (*4*). The biosynthetic pathway for DPG consists of five enzymes present in the producer gene cluster (*2*). The enzyme DpgA, a type III polyketide synthase, couples four molecules of malonylcoenzyme A, and DpgB/DpgD catalyze the subsequent dehydration to form (3,5-dihydroxyphenylacetyl)-coenzyme A (DPA-CoA, **3**). DpgC then adds dioxygen and cleaves the thioester bond to generate DPGX (3,5-dihydroxyphenylglyoxylate, **4**; Figure 1B) and coenzyme A (CoA). In the final step of the pathway, a promiscuous PLP-dependent transaminase (HpgT) converts the α-keto acid DPGX to the amino acid DPG (*5*).

DpgC performs a mechanistically complex transformation encompassing both the four-electron oxidation of the benzylic carbon of the substrate DPA-CoA (**3**) and formal hydrolysis of the thioester bond to generate free CoA. Isotopic labeling studies established that DpgC is a dioxygenase, incorporating both oxygen atoms from molecular oxygen into the substrate. A variety of biochemical experiments demonstrated that catalytic activity is independent of metal ions or cofactors, making this enzyme an unusual oxygenase (*1*). The majority of characterized oxygenases exploit bound transition metals, primarily iron/copper, or flavin/pterin cofactors to activate triplet dioxygen to carry out oxidation chemistry (*6*). The direct reaction of molecular oxygen with organic molecules is formally a disallowed, spin-forbidden process (*7*). Besides DpgC, there are few characterized dioxygenases with activity independent of cofactors, namely, the related 1*H*-3-hydroxy-4-oxoquinaldine-2,4-dioxygenase (Hod) and 1*H*-3-hydroxy-4-oxoquinoline-2,4-dioxygenase (Qdo), both involved in quinolone degradation (*8*, *9*). There are limited examples of cofactor/metal-free monooxygenases including the quinone-forming monooxygenases involved in tailoring polyketides and urate oxidase (*10*−*12*). In addition, there are documented examples of enzymes catalyzing cofactor-independent addition of oxygen as side reactions of anionic intermediates (*13*). On the basis of previous biochemical and mechanistic analyses, the mechanism of cofactor-independent oxygenases is believed to proceed through electron-rich intermediates followed by single-electron transfers to dioxygen (*7*). This

[†] This work was supported in part by funds from Boston College and the Damon Runyon Cancer Research Foundation (Grant DRS-41-01).

[‡] Coordinates have been deposited within the Protein Data Bank (PDB code 2PG8).

* To whom correspondence should be addressed. Phone: (617) 552-2931. Fax: (617) 552-2705. E-mail: bruner@bc.edu.

[1] Abbreviations: DPG, 3,5-dihydroxyphenylglycine; NRPS, nonribosomal peptide synthetase; CoA, coenzyme A; DPA-CoA, (3,5-dihydroxyphenylacetyl)coenzyme A; DPA-NH-CoA, (3,5-dihydroxyphenylacetyl)aminodesulfocoenzyme A; DPGX, 3,5-dihydroxyphenylglyoxylate; PLP, pyridoxal 5′-phosphate; LB, Luria−Bertani medium; IPTG, isopropyl β-D-thiogalactopyranoside; Ni-NTA, nickel nitrilotriacetic acid; DTNB, 5,5′-dithiobis(2-nitrobenzoic acid); TFA, trifluoroacetic acid; PEG, polyethylene glycol; NCS, noncrystallographic symmetry; DHP, 3,5-dihydroxyphenyl.

10.1021/bi701148b CCC: $37.00
Published on Web 11/16/2007

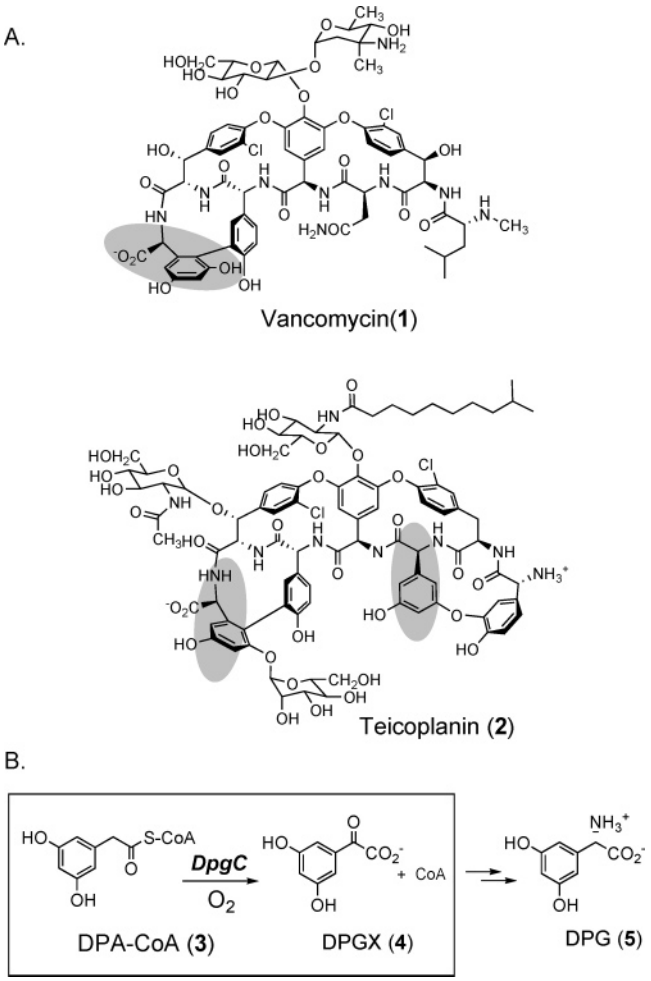

FIGURE 1: Biosynthesis of the nonproteinogenic amino acid DPG: (A) structures of the antibiotics vancomycin (**1**) and teicoplanin (**2**) with the amino acid DPG highlighted, (B) overall reaction catalyzed by the cofactor-independent dioxygenase DpgC.

general mechanistic pathway is analogous to that proposed for the reaction of molecular oxygen with reduced flavin cofactors (*14*).

We have previously described the X-ray crystal structure of a complex between DpgC and an isosteric synthetic substrate analogue (*15*). The designed inhibitor (DPA-NH-CoA) differs from the substrate DPA-CoA (see Figure 1, **3**) only by the substitution of an amide for the natural thioester (*16*). This change produces a nonhydrolyzable CoA thioester analogue and raises the pK_a of the benzylic hydrogens, allowing the analogue to be completely inert to the chemistry of DpgC. The use of this synthetic substrate analogue in X-ray cocrystallization experiments provided an accurate approximation of the enzyme/substrate complex and allowed insights into the mechanism of substrate recognition and catalysis. This work also established DpgC as a structural homologue to the crotonase, enoyl-CoA isomerase/dehydratase superfamily (*15*). Members of this diverse enzyme family perform a wide variety of chemical transformations on acylcoenzyme A substrates; however, DpgC is the only example of oxidation chemistry from this family (*17*−*21*). These enzymes process acyl-CoA substrates primarily through stabilization of intermediate thioester enolates (*17*, *18*). As observed with other crotonase homologues, DpgC makes several specific interactions with the 3′-phospho-5′-diphosphoadenosine moiety of the substrate that contributes

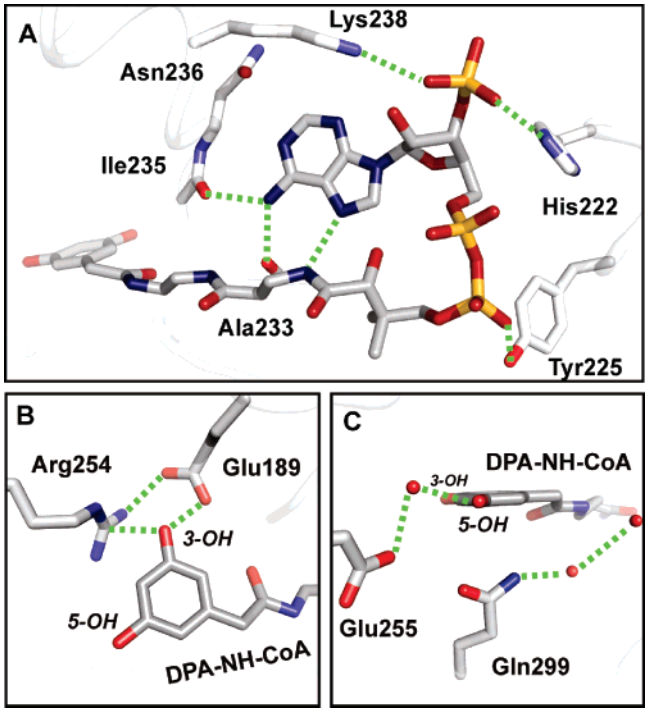

FIGURE 2: Substrate interactions between DpgC and the stable amide analogue of the substrate DPA-NH-CoA (PDB code 2NP9): (A) conformation and binding contacts of DPA-NH-CoA shown in gray with amino acid side chains of DpgC (white), (B) specific interactions between the enzyme and the phenol of the substrate, (C) ordered water molecules (red spheres) present in the active site of DpgC.

a significant portion of the binding interactions. The CoA substrate bends back on itself (Figure 2A), with the N7 of adenosine forming a hydrogen bond with the amide group of the pantetheine portion of DPA-CoA. Interactions between DpgC and DPA-CoA include phosphate contacts from Lys238, His222, and Tyr225. In addition, the backbone amide carbonyls of Ala233 and Ile235 form bidentate hydrogen bonds with the exocyclic amine of the adenine base.

Enzyme/substrate interactions specific to the chemistry of DpgC are centered at the 3,5-dihydroxyphenylacetyl thioester of the substrate. Four amino acid side chains (Glu189, Arg254, Glu255, and Gln299) are in proximity to the 3,5-dihydroxyphenyl ring of the substrate DPA-CoA (*15*). Each of the residues is absolutely conserved in the five known DpgC homologues on the basis of sequence alignment (*22*−*26*). There is, however, no significant overlap between these four conserved active site residues of DpgC and other crotonase family members (*20*, *27*−*31*). This suggests these residues are unique to the oxidation chemistry of DpgC. One of the two symmetric phenol hydroxyls (designated 3-OH, Figure 2B) interacts specifically with two enzyme side chains, Arg254 and Glu189. The oxygen of the 3-OH is also in close proximity to the planar face of the Arg254 guanidinium group. This is an atypical interaction as the phenolic oxygen is nearest (3.3 Å) to the carbon of the positively charged guanidinium group and orthogonal to the NH hydrogen bond donors (Figure 2B). In the majority of observed interactions between arginine residues and hydrogen bond acceptors or anions, the guanidium group forms hydrogen bonds with the electronegative functionality. This includes a large number of documented arginine/phosphate

interactions (*32*). When interacting with aromatic amino acids, the guanidinium group of arginine tends to stack with aromatic rings, but they also can interact in an edge/face orientation (*33*). Also in proximity to this phenol is the carboxylate group of Glu189, which forms a bidentate hydrogen bond with 3-OH and with a guanidinium NH of Arg254 (hydrogen-bonding distances of 2.4 and 2.8 Å, respectively), implying the hydrogen of the phenol is between the substrate and Glu189 (Figure 2B).

The combined results from structural and biochemical experiments led to a mechanistic proposal where the substrate binds to the enzyme as the thioester enolate with an adjacent bound oxygen molecule (*1*, *15*). In a two-step reaction analogous to the reaction of oxygen with flavin cofactors, the substrate transfers an electron to dioxygen, forming a radical pair which can collapse in a C−O bond-forming reaction. Here we report the use of site-directed mutagenesis, biochemical analysis of alternate substrates, and X-ray crystallographic structure determination to probe the enzyme and substrate determinants for binding and catalysis by DpgC.

MATERIALS AND METHODS

Site-Directed Mutagenesis. Amino acid point mutations of DpgC were made using the QuikChange site-directed mutagenesis kit (Stratagene, La Jolla, CA). DpgC from the *Streptomyces toyocaensis* A47934 gene cluster cloned into the vector pET30a was used as the template (*15*). PCR amplification was performed following the manufacturer's protocol with the following primers and their reverse complements (modified sequences underlined): Glu189Gln, 5′-CGC CTG AAC GCC CAG GAC GGT CAG CAG-3′; Arg254Lys, 5′-GTC GAC TTC CTG ATG CGC AAG GAA CTC GGC TAC-3′; Glu255Gln, 5′-TTC CTG ATG CGC CGG CAA CTC GGC TAC ATC-3′; Gln299Glu, 5′-GGC GGC GGA GCC AAC TTG CTG CTG GTC-3′. The oligonucleotides were synthesized by Integrated DNA Technologies (Coralville, IA). The PCR program consisted of an initial hold of 95 °C for 1 min followed by 30 cycles of 95 °C for 1 min, 55 °C for 1 min, and 65 °C for 13.5 min. The template DNA was digested with 10 U of *Dpn*I for 1 h at 37 °C before transformation into XL10-Gold Ultracompetent cells. The mutagenesis products were confirmed by DNA sequencing.

DpgC Mutant Expression and Purification. BL21(DE3) *Escherichia coli* cells were transformed with mutant vectors and grown in LB medium at 37 °C until the cell density reached $OD_{600} = 0.6$. Overexpression was induced by adding IPTG (50 μM), followed by overnight incubation at 18 °C. Cells were pelleted using centrifugation and lysed using a French press system. The enzymes were then purified with Ni-NTA affinity resin (Qiagen), dialyzed into a common buffer (20 mM Tris·HCl, 50 mM NaCl, pH 7.5), concentrated, flash frozen in buffer with 20% glycerol, and stored at −80 °C.

Enzyme Activity Assays. Kinetic analysis for DpgC mutants was performed using the DTNB [5,5′-dithiobis(2-nitrobenzoic acid)] reporter assay as described (*1*, *15*) with one modification: the concentration of DpgC mutants used was 0.19 μM. To determine the kinetic parameters of DpgC mutants for substrate DPA-CoA, a freshly prepared solution of DTNB (1 mM), Tris·HCl, pH 7.5 (250 mM), and increasing concentrations of DPA-CoA was mixed with DpgC (0.19 μM) at 24 °C (100 μL). The reactions were continually monitored with a UV−vis spectrophotometer at 412 nm for 5 min. For oxygen-saturated buffer assays, the conditions were identical to those described above with the exception that oxygen gas was rigorously bubbled through the buffers for 5 min.

Synthesis of DPA-CoA Substrate Analogues. The general coupling procedure of the phenylacetic acid derivatives with coenzyme A follows published procedures for the synthesis of substrate DPA-CoA (*1*, *15*).

(1) Phenylacetyl-CoA. Potassium carbonate (7 mg) was added to a solution of phenylacetic acid (4.4 mg, 2.5 equiv), PyBOP (16.9 mg, 2.5 equiv), and CoA (10 mg, 1 equiv) in 1 mL of 1:1 THF/H_2O. The reaction was stirred for 2 h at room temperature followed by acidification with 1 μL of TFA. The solution was flash frozen in liquid N_2 and lyophilized to dryness. The crude product was purified by preparative HPLC using a Vydac 218TP1022 C18 column (8 mL/min; 0−3 min, 2% B; 3−40 min, 5−15% B; A = 0.1% TFA/H_2O and B = CH_3CN; phenylacetyl-CoA eluted at 36 min), monitoring at 260 nm. Removal of the solvents by lyophilization gave phenylacetyl-CoA as a white powder (9 mg, yield 80%). Compounds were stored at −20 °C. ^{1}H NMR spectra of all compounds were taken on a Varian 400 MHz NMR instrument in D_2O. The following are data for phenylacetyl-CoA. ^{1}H NMR: δ 8.61 (s, 1H), 8.35 (s, 1H), 7.25 (overlapping m, 5H), 6.16 (d, 1H), 4.58 (overlapping m, 3H), 4.62 (br s, 1H), 3.91 (s, 1H), 3.85 (d, 1H), 3.70 (m, 4H), 3.60 (d, 1H), 3.28 (m, 4H), 2.96 (t, 2H), 2.23 (t, 2H), 0.92 (s, 3H), 0.79 (s, 3H). ES+ TOF MS: *m*/*z* 907.2 (907.5 calcd, $C_{29}H_{41}N_7O_{17}P_3SNa$).

(2) 4-Hydroxyphenylacetyl-CoA. HPLC purification: 8 mL/min; 0−3 min, 2% B; 3−40 min, 2−60% B; A = 0.1% TFA/H_2O and B = CH_3CN; 4-hydroxyphenylacetyl-CoA eluted at 17 min. ^{1}H NMR: δ 8.64 (s, 1H), 8.39 (s, 1H), 7.11 (d, 2H), 6.77 (d, 2H), 6.19 (d, 1H), 4.88 (overlapping m, 4H), 4.60 (br s, 1H), 4.27 (br s, 2H), 4.02 (s, 1H), 3.87 (m, 1H), 3.61 (m, 1H), 3.78 (overlapping m, 4H), 3.33 (overlapping m, 4H), 2.99 (t, 2H), 2.26 (t, 2H), 0.93 (s, 3H), 0.79 (s, 3H). ES+ TOF MS: *m*/*z* 923.2 (923.5 calcd, $C_{29}H_{41}N_7O_{18}P_3SNa$).

(3) 3-Hydroxyphenylacetyl-CoA. HPLC purification: 8 mL/min; 0−3 min, 2% B; 3−40 min, 2−60% B; A = 0.1% TFA/H_2O and B = CH_3CN; 3-hydroxyphenylacetyl-CoA eluted at 37 min. ^{1}H NMR: δ 8.61 (s, 1H), 8.36 (s, 1H), 7.15 (t, 1H), 6.76−6.70 (overlapping m, 3H), 6.17 (d, 1H), 4.88 (overlapping m, 4H), 4.60 (br s, 1H), 4.28 (br s, 2H), 4.00 (s, 1H), 3.87 (m, 1H), 3.81 (s, 1H), 3.71 (overlapping m, 4H), 3.61 (m, 1H), 3.30 (overlapping m, 4H), 2.98 (t, 2H), 2.26 (t, 2H), 0.92 (s, 3H), 0.79 (s, 3H). ES+ TOF MS: *m*/*z* 923.2 (923.5 calcd, $C_{29}H_{41}N_7O_{18}P_3SNa$).

DPA-S-(N-acetylcysteamine) was synthesized using a published procedure (*34*), and the crude product was purified via preparative HPLC using a Vydac 218TP1022 C18 column (8 mL/min; 0−3 min, 10% B; 3−50 min, 10−40% B; A = 0.1% TFA/H_2O and B = CH_3CN; DPA-SNAC eluted at 21.5 min), monitoring at 260 and 220 nm. Concentration by rotary evaporation and lyophilization gave DPA-*S*-(*N*-acetylcysteamine) as a white powder. ^{1}H NMR: δ 6.38 (d, 2H), 6.33 (t, 1H), 3.79 (s, 2H), 3.33 (t, 2H), 3.03

(t, 2H), 1.8 (s, 1H); ES+ TOF MS: *m*/*z* 292.6 (292.3 calcd, $C_{12}H_{15}NO_4SNa$). DPA-*S*-(*N*-acetylcysteamine) (in varying concentrations, 0.5−3.0 mM) was incubated with DpgC (2.5 μM) at 24 °C (100 μL, 20 mM Tris·HCl, pH 7.5) for 1 h. The reaction was quenched with 1 μL of TFA, and the products were analyzed by analytical C18 HPLC (1 mL/min; 0−3 min, 2% B; 3−40 min, 2−30% B; A = 0.1% TFA/H_2O and B = 0.1% TFA/CH_3CN), monitoring at 260 and 220 nm.

Crystallization, Data Collection, and Structure Determination. Arg254Lys-DpgC (48 kDa, 439 amino acids) was cocrystallized with the substrate analogue DPA-NH-CoA by the hanging-drop method at 20 °C. DPA-NH-CoA (2 mM) was incubated with Arg254Lys-DpgC (12 mg/mL in 20 mM Tris·HCl and 50 mM NaCl, pH 7.5) at 20 °C for 2 h. The DpgC/DPA-NH-CoA complex (1.5 μL) was mixed with 1.5 μL of reservoir solution: 100 mM sodium citrate, 150 mM ammonium acetate, and 15% (w/v) PEG 4000, pH 5.6. Crystals appeared after 2 days at 20 °C. The crystals were transferred to a cryoprotectant solution (reservoir solution with 20% glycerol) and soaked for 30 min before being flash frozen in liquid nitrogen. Diffraction data were collected to 3.0 Å at the X12C beamline of the National Synchrotron Light Source (NSLS) at Brookhaven National Laboratory. Diffraction data were processed and scaled with the program package HKL2000 (*35*). The crystal structure was solved by molecular replacement using the program CNS (*36*) with native DpgC as the search model (PDB entry 2NP9). Refinement of the structure was performed with NCS restraints using the program CNS. As with the wild-type structure, only three of the six monomers were ordered in the crystal, resulting in an $R_{working} = 0.33$ and $R_{free} = 0.36$ (*15*). The program PyMOL (Delano Scientific, San Carlos, CA) was used to generate graphic images.

RESULTS AND DISCUSSION

Recognition of the Substrate DPA-CoA by DpgC. to confirm the importance of the entire CoA moiety in the chemistry and substrate binding of DpgC, the truncated DPA-*S*-(*N*-acetylcysteamine) was prepared and assayed. *N*-Acetylcysteamine analogues of CoA thioesters are frequently used as substrate mimics for a variety of CoA and phosphopantetheinyl utilizing enzymes as these compounds are structurally analogous to the section of the substrate involved directly in the enzyme chemistry (*34*, *37*−*39*). DpgC was incubated with concentrations of DPA-*S*-(*N*-acetylcysteamine) up to 3 mM; however, enzyme activity was not observed under any conditions (data not shown). This confirms the necessity of the 3′-phospho-5′-diphosphoadenosine moiety of the substrate in the chemistry of DpgC.

As described in the introduction, the structure of DpgC bound to the substrate analogue DPA-NH-CoA placed four residues in position to interact with the phenylacetyl portion of the substrate and be directly involved in the oxidation chemistry. To dissect the roles these residues play in substrate recognition and catalysis, we used site-directed mutagenesis to alter the functionalities and evaluate the effects by measuring the kinetic parameters of the reaction.

Mutation of either Arg254 or Glu189 had a strong affect on the activity of the enzyme (Table 2, entries 2 and 3). The sterically conservative mutation Glu189Gln was used to probe the importance of the hydrogen bond to 3-OH observed in the structure of DpgC (Figure 2B). The Glu189Gln construct had a measured K_M value ∼20 times higher than that of the wild-type enzyme, indicating that the anionic side chain of Glu189 is important for substrate binding. The role of the unusual arginine interaction with the same substrate 3-OH was probed by mutation of arginine to lysine. This change places a positively charged, hydrogen bond donor ($-NH_3^+$) in a favorable position to interact with the 3-OH as observed with Arg254. The mutation had a dramatic affect on the Michaelis constant, suggesting the substrate binds with ∼50 times lower affinity. Both mutations had only a modest effect on the enzyme turnover rate, with activity measured at approximately half the rate measured for wild-type DpgC. The presented measurements were conducted under physiologically relevant, ambient oxygen concentrations. To assess the effect oxygen concentration has on the kinetics, measurements were also performed in oxygen-saturated buffers. In all cases, the increase in oxygen concentration had little effect (within 2%) on the measured k_{cat}/K_M at 1 atm.

To further address the substantial change in enzyme activity of Arg254Lys, we solved the X-ray crystal structure of this construct bound to the substrate analogue DPA-NH-CoA. The structure will both provide a basis for the observed decrease in enzyme activity and rule out the possibility of a global structural change. The complex crystallized under the same conditions and space group symmetry as the wild-type enzyme complex. The structure was solved using the phase information from the wild-type co-complex (PDB entry

Table 1: Data Collection and Refinement Statistics for R254K DpgC

Data Collection	
space group	$P2_12_12$
cell dimensions	
a, *b*, *c* (Å)	139.054, 155.309, 169.208
α, *β*, *γ* (deg)	90, 90, 90
wavelength	1.000
resolution (Å)	3.0
R_{sym} or R_{merge} (high-resolution shell)	0.116 (0.593)
$I/\sigma(I)$	7.4
completeness (%)	99
redundancy	9.8
Refinement	
resolution (Å)	2.6
no. of reflns	69142
R_{work}/R_{free}	0.331, 0.367
no. of atoms	
protein	9619
ligand/ion	177
water	123
rms dev	
bond lengths (Å)	0.010 (0.008)
bond angles (deg)	1.5 (1.4827)

Table 2: Kinetic Parameters for DpgC Mutant Enzymes with the Natural Substrate DPA-CoA

entry	enzyme	K_M (μM)	k_{cat} (min^{-1})	k_{cat}/K_M[a]
1	wild type	3.9 ± 0.6	10.32 ± 0.42	1 (1.022)
2	Arg254Lys	217 ± 46	5.17 ± 0.32	0.009 (0.014)
3	Glu189Gln	64 ± 13	5.12 ± 0.41	0.029
4	Glu255Gln	3.6 ± 1.9	9.18 ± 0.78	0.959
5	Gln299Asn	2.5 ± 1.1	4.14 ± 0.21	0.619

[a] Relative apparent second-order rate constants. Measurements performed with oxygen-saturated buffer are shown in parentheses.

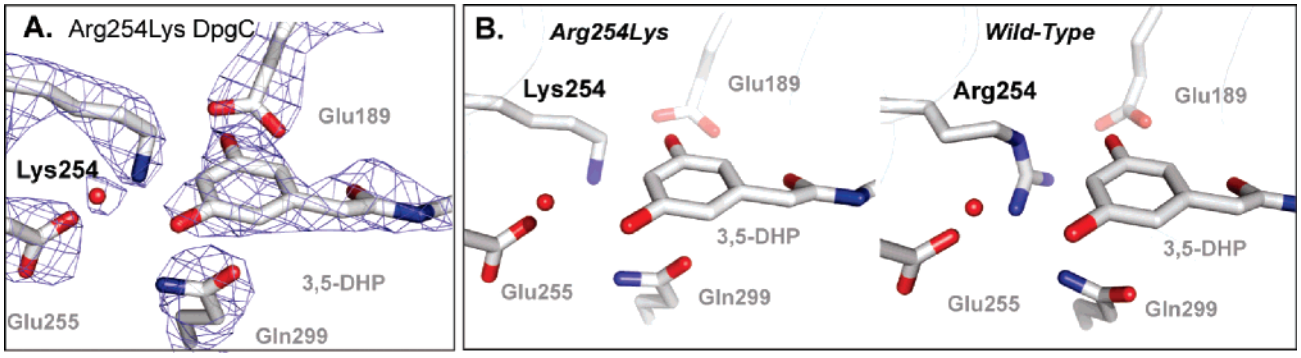

FIGURE 3: X-ray crystal structure of Arg254Lys DpgC. (A) Electron density map of the region around the substrate analogue DPA-NH-CoA. The $2F_o - F_c$ map is contoured to 1.3 σ at a resolution of 3.0 Å. (B) Side-by-side comparison of Arg254Lys with wild-type DpgC in the same orientation.

2NP9), and the lysine mutation was built into the model. The entire structure was then subjected to several rounds of refinement (Table 1). As diagrammed in Figure 3, the active site conformation of Arg254Lys deviates very little from that of the wild-type enzyme (rmsd over all atoms 0.52 Å). The substrate analogue is bound in the same orientation as observed for the wild-type enzyme, and electron density consistent with molecular oxygen is evident adjacent to the substrate analogue. The ammonium group of lysine is positioned to make a favorable electrostatic interaction with the 3-OH of the substrate, though the distance (3.3 Å) and geometry are not optimal to make a hydrogen bond. However, no constraints are evident in the structure to prevent formation of this hydrogen bond. The results confirm that the specific chemical configuration of the arginine is important for activity and the interaction observed in the wild-type enzyme is not a simple electrostatic/hydrogen-bonding interaction.

The lysine of Arg254Lys DpgC is not, however, in position to hydrogen bond with Glu189, which forms an interaction with the substrate 3-OH in the wild-type enzyme (see Figure 3B). In this case, the phenol must be acting as a hydrogen bond donor. As neither of the conservative mutations of Arg254 or Glu189 is likely to exert a global negative effect on substrate binding, the dyad plays an important role in catalysis and is the major determinant for binding the 3,5-dihydroxyl ring of the substrate.

Two additional residues are observed in the active site pocket of DpgC within close proximity to the 3,5-dihydroxyphenyl ring of the substrate. Glu255 and Gln299 both form water-mediated interactions with the substrate and were proposed to play a role in the catalytic cycle (*15*). Glu255 forms the only observed interaction with the 5-hydroxyl of DPA-CoA (5-OH, Figure 2C) through an intervening water molecule. Mutation of this residue to glutamine resulted in an enzyme that retains activity similar to that of the wild type (Table 2, entry 3), suggesting specific recognition of the 5-OH is not important for enzyme function.

On the basis of homology to the crotonase family of enzymes, an early step in the catalytic cycle of DpgC is likely the formation of a thioester enolate. As observed for most members of this enzyme family, two backbone amides act as hydrogen bond donors to stabilize the enolate through an interaction analogous to that of the oxyanion hole of hydrolase enzymes (*40*). In the case of DpgC, the backbone amides of residues Gly235 and Ile296 are properly oriented to form hydrogen bonds with the thioester of the substrate. There is no amino acid derived general base to directly assist in the deprotonation of an α-hydrogen in the substrate. However, there is an ordered water molecule positioned adjacent to the proR α-hydrogen predicted to be the acidic hydrogen. As observed with other crotonase family members, catalysis in DpgC is driven by stabilization of thioester enolate through a tight binding interaction (*17*, *18*). For example, coenzyme A acyl thioesters bound to the enoyl-CoA hydratase crotonase have a measured pK_a of ~8.5 (*41*). The substrate of DpgC contains an α-phenyl ring that will further lower the pK_a of the substrate. Taken together, the pK_a of DPA-CoA bound in the active site of DpgC can be estimated to be <7.5, and therefore, a specific enzyme-associated base is not necessary. The role of the network of waters anchored by Gln299 could function to provide a mechanism to shuttle the two protons produced during the catalytic cycle to bulk solvent. To test this hypothesis, the mutant Gln299Asn was constructed and biochemically characterized. The change resulted in a 2-fold reduction to the overall k_{cat}/K_M as compared to that of the wild-type enzyme. This effect was largely a consequence of a reduction in the rate of catalysis, supporting the importance of the structurally observed water molecule in facilitating the formation of the thioester enolate.

Phenylacetyl-CoA analogues were synthesized and assayed against the wild-type enzyme to examine the role substrate functional groups play in the chemistry of DpgC. In particular, the two symmetric phenol groups (3-OH and 5-OH) of the substrate were probed. Various CoA thioester substrate analogues were prepared by coupling phenylacetic acid derivatives to coenzyme A using PyBOP condensation chemistry (*1*, *15*). The products of the reaction were purified to homogeneity using preparative HPLC, and kinetic parameters were determined using wild-type DpgC. The site-directed mutagenesis data discussed above implicate that one of the two hydroxyls is important for both catalysis and binding of the substrate. We tested three substrate analogues that varied in the substitution pattern of the phenyl ring with the wild-type enzyme. In general, as shown in Table 3, DpgC has the ability to process a diverse range of substituted phenylacetyl-CoA substrates. Removal of one of the hydroxyl groups from the natural substrate (3-hydroxyphenylacetyl-CoA, entry 2) had little effect on the activity of the enzyme in terms of both the measured k_{cat} and the measured K_M. However, phenylacetyl-CoA lacking both hydroxyls (entry

Table 3: Evaluation of the Activity of Alternate Phenylacetyl-CoA Substrates for DpgC

entry	substrate	K_M (μM)	k_{cat} (min^{-1})	k_{cat}/K_M*
1	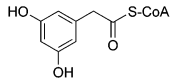	3.9 ± 0.6	10.32 ± 0.36	1 (1.022)
2	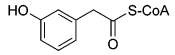	4.4 ± 1.4	7.52 ± 0.57	0.650 (0.558)
3	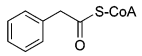	102 ± 37	3.84 ± 0.36	0.014
4	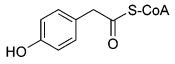	851 ± 361	13.32 ± 2.33	0.006

[a] Relative apparent second-order rate constants. Measurements performed with oxygen-saturated buffer are shown in parentheses.

Scheme 1

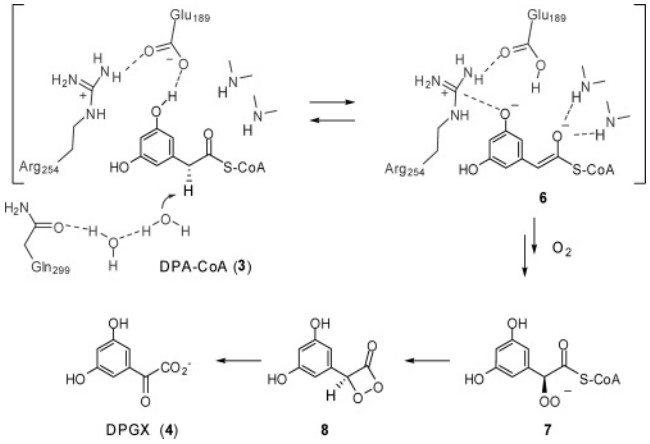

3) was less efficiently processed by DpgC. Repositioning a hydroxyl to the 4-position (4-hydroxyphenylacetyl-CoA, entry 4) gave a substrate that was still turned over by the enzyme, but with much lower efficiency (as measured by the relative k_{cat}/K_M values). Interestingly, the substrate analogue with a hydroxyl in the 4-position had a substantially weaker binding but a k_{cat} slightly faster than those of the the natural substrate. The presence of a 4-hydroxyl group could influence the electronics of the enzyme-bound enolate by increasing the electron density at the benzylic position and facilitating the downstream reaction with molecular oxygen despite the large negative affect on substrate binding.

Crystals of the co-complexes between DpgC and both phenyl and 4-hydroxyphenylacetyl-NH-CoA were grown and the structures determined. Electron density corresponding to these analogues, however, was difficult to interpret, and the phenyl rings appeared to be bound in multiple confirmations (data not shown).

Overall this work supports a mechanism of substrate recognition and catalysis by DpgC as illustrated in Scheme 1. The substrate binds to the enzyme in the amide backbone oxyanion hole, and equilibration to the thioester enolate is facilitated by an ordered water molecule. Molecular oxygen then reacts with the benzylic carbon. Experiments on cofactor-independent oxygenases and flavoenzymes predict reaction with molecular oxygen proceeds through an electron-rich substrate intermediate (*7*−*9*, *11*, *14*, *43*, *44*). An analogous scheme can be envisioned for DpgC with an intermediate conjugated enolate. Our results suggest interactions between Arg254/Glu189 and the substrate 3-OH play an important function in catalysis. One possible role could be to increase the electron density of the conjugated intermediate by forming a partial or full (as illustrated in Scheme 1, **6**) negative charge on this hydroxyl. The specific role of the atypical interaction of Arg254 could be necessary to stabilize the negative charge while not presenting an acidic proton to the phenoxide **6**. This scenario would predict an increase in the pK_a of Glu189 caused by the enzyme environment. Supporting this, Glu189 is in a hydrophobic region of the structure, within 6 Å of the side chains of Ile235, Phe250, Leu300, and Val194. An enzyme-bound dianion would facilitate electron transfer to molecular oxygen, forming superoxide. Dioxygen is bound in the active site adjacent to the benzylic carbon in a small hydrophobic binding pocket (*15*). This orientation places dioxygen in close proximity to react with the intermediate **6** through a two-step single-electron process, forming the peroxidate **7**. The details of the final two steps have not been established, but can be predicted to proceed through analogous "oxyanion hole" chemistry as described for the initial thioester enolate formation.

ACKNOWLEDGMENT

We thank the staff at the Brookhaven NSLS PXRR for assistance with X-ray data collection. We are grateful to members of the Bruner laboratory for comments on the manuscript and helpful discussions.

REFERENCES

1. Tseng, C. C., Vaillancourt, F. H., Bruner, S. D., and Walsh, C. T. (2004) DpgC is a metal- and cofactor-free 3,5-dihydroxyphenylacetyl-CoA 1,2-dioxygenase in the vancomycin biosynthetic pathway, *Chem. Biol. 11*, 1195−1203.
2. Chen, H., Tseng, C. C., Hubbard, B. K., and Walsh, C. T. (2001) Glycopeptide antibiotic biosynthesis: enzymatic assembly of the dedicated amino acid monomer (*S*)-3,5-dihydroxyphenylglycine, *Proc. Natl. Acad. Sci. U.S.A. 98*, 14901−14906.
3. Hubbard, B. K., and Walsh, C. T. (2003) Vancomycin assembly: nature's way, *Angew. Chem., Int. Ed. 42*, 730−765.
4. Barna, J. C., and Williams, D. H. (1984) The structure and mode of action of glycopeptide antibiotics of the vancomycin group, *Annu. Rev. Microbiol. 38*, 339−357.
5. Hubbard, B. K., Thomas, M. G., and Walsh, C. T. (2000) Biosynthesis of L-*p*-hydroxyphenylglycine, a non-proteinogenic amino acid constituent of peptide antibiotics, *Chem. Biol. 7*, 931−942.
6. Silverman, R. B. (2002) *The Organic Chemistry of Enzyme-Catalyzed Reactions*, revised edition, Academic Press, San Diego.
7. Fetzner, S. (2002) Oxygenases without requirement for cofactors or metal ions, *Appl. Microbiol. Biotechnol. 60*, 243−257.
8. Frerichs-Deeken, U., Ranguelova, K., Kappl, R., Huttermann, J., and Fetzner, S. (2004) Dioxygenases without requirement for cofactors and their chemical model reaction: compulsory order ternary complex mechanism of 1*H*-3-hydroxy-4-oxoquinaldine 2,4-dioxygenase involving general base catalysis by histidine 251 and single-electron oxidation of the substrate dianion, *Biochemistry 43*, 14485−14499.
9. Frerichs-Deeken, U., and Fetzner, S. (2005) Dioxygenases without requirement for cofactors: identification of amino acid residues involved in substrate binding and catalysis, and testing for rate-limiting steps in the reaction of *1H*-3-hydroxy-4-oxoquinaldine 2,4-dioxygenase, *Curr. Microbiol. 51*, 344−352.
10. Shen, B., and Hutchinson, C. R. (1993) Tetracenomycin F1 monooxygenase: oxidation of a naphthacenone to a naphthacenequinone in the biosynthesis of tetracenomycin C in *Streptomyces glaucescens*, *Biochemistry 32*, 6656−6663.

11. Sciara, G., Kendrew, S. G., Miele, A. E., Marsh, N. G., Federici, L., Malatesta, F., Schimperna, G., Savino, C., and Vallone, B. (2003) The structure of ActVA-Orf6, a novel type of monooxygenase involved in actinorhodin biosynthesis, *EMBO J. 22*, 205−215.
12. Colloc'h, N., el Hajji, M., Bachet, B., L'Hermite, G., Schiltz, M., Prange, T., Castro, B., and Mornon, J. P. (1997) Crystal structure of the protein drug urate oxidase-inhibitor complex at 2.05 Å resolution, *Nat. Struct. Biol. 4*, 947−952.
13. Abell, L. M., and Schloss, J. V. (1991) Oxygenase side reactions of acetolactate synthase and other carbanion-forming enzymes, *Biochemistry 30*, 7883−7887.
14. Massey, V. (1994) Activation of molecular oxygen by flavins and flavoproteins, *J. Biol. Chem. 269*, 22459−22462.
15. Widboom, P., Fielding, E. N., Liu, Y., and Bruner, S. D. (2007) Structural basis for cofactor-independent dioxygenation in vancomycin biosynthesis, *Nature 447*, 342−345.
16. Liu, Y., and Bruner, S. D. (2007) Rational manipulation of carrier-domain geometry in nonribosomal peptide synthetases, *ChemBioChem 8*, 617−621.
17. Holden, H. M., Benning, M. M., Haller, T., and Gerlt, J. A. (2001) The crotonase superfamily: divergently related enzymes that catalyze different reactions involving acyl coenzyme a thioesters, *Acc. Chem. Res. 34*, 145−157.
18. Agnihotri, G., and Liu, H. W. (2003) Enoyl-CoA hydratase. Reaction, mechanism, and inhibition, *Bioorg. Med. Chem. 11*, 9−20.
19. Gerratana, B., Arnett, S. O., Stapon, A., and Townsend, C. A. (2004) Carboxymethylproline synthase from *Pectobacterium carotorova*: a multifaceted member of the crotonase superfamily, *Biochemistry 43*, 15936−15945.
20. Truglio, J. J., Theis, K., Feng, Y., Gajda, R., Machutta, C., Tonge, P. J., and Kisker, C. (2003) Crystal structure of Mycobacterium tuberculosis MenB, a key enzyme in vitamin K2 biosynthesis, *J. Biol. Chem. 278*, 42352−42360.
21. Eberhard, E. D., and Gerlt, J. A. (2004) Evolution of function in the crotonase superfamily: the stereochemical course of the reaction catalyzed by 2-ketocyclohexanecarboxyl-CoA hydrolase, *J. Am. Chem. Soc. 126*, 7188−7189.
22. Sosio, M., Bianchi, A., Bossi, E., and Donadio, S. (2000) Teicoplanin biosynthesis genes in *Actinoplanes teichomyceticus*, *Antonie Van Leeuwenhoek 78*, 379−384.
23. Pelzer, S., Sussmuth, R., Heckmann, D., Recktenwald, J., Huber, P., Jung, G., and Wohlleben, W. (1999) Identification and analysis of the balhimycin biosynthetic gene cluster and its use for manipulating glycopeptide biosynthesis in *Amycolatopsis mediterranei* DSM5908, *Antimicrob. Agents Chemother. 43*, 1565−1573.
24. van Wageningen, A. M., Kirkpatrick, P. N., Williams, D. H., Harris, B. R., Kershaw, J. K., Lennard, N. J., Jones, M., Jones, S. J., and Solenberg, P. J. (1998) Sequencing and analysis of genes involved in the biosynthesis of a vancomycin group antibiotic, *Chem. Biol. 5*, 155−162.
25. Pootoolal, J., Thomas, M. G., Marshall, C. G., Neu, J. M., Hubbard, B. K., Walsh, C. T., and Wright, G. D. (2002) Assembling the glycopeptide antibiotic scaffold: The biosynthesis of A47934 from *Streptomyces toyocaensis* NRRL15009, *Proc. Natl. Acad. Sci. U.S.A. 99*, 8962−8967.
26. Sosio, M., Stinchi, S., Beltrametti, F., Lazzarini, A., and Donadio, S. (2003) The gene cluster for the biosynthesis of the glycopeptide antibiotic A40926 by Nonomuraea species, *Chem. Biol. 10*, 541−549.
27. Sleeman, M. C., Sorensen, J. L., Batchelar, E. T., McDonough, M. A., and Schofield, C. J. (2005) Structural and mechanistic studies on carboxymethylproline synthase (CarB), a unique member of the crotonase superfamily catalyzing the first step in carbapenem biosynthesis, *J. Biol. Chem. 280*, 34956−34965.
28. Koski, K. M., Haapalainen, A. M., Hiltunen, J. K., and Glumoff, T. (2005) Crystal structure of 2-enoyl-CoA hydratase 2 from human peroxisomal multifunctional enzyme type 2, *J. Mol. Biol. 345*, 1157−1169.
29. Benning, M. M., Haller, T., Gerlt, J. A., and Holden, H. M. (2000) New reactions in the crotonase superfamily: structure of methylmalonyl CoA decarboxylase from *Escherichia coli*, *Biochemistry 39*, 4630−4639.
30. Whittingham, J. L., Turkenburg, J. P., Verma, C. S., Walsh, M. A., and Grogan, G. (2003) The 2-A crystal structure of 6-oxo camphor hydrolase. New structural diversity in the crotonase superfamily, *J. Biol. Chem. 278*, 1744−1750.
31. Modis, Y., Filppula, S. A., Novikov, D. K., Norledge, B., Hiltunen, J. K., and Wierenga, R. K. (1998) The crystal structure of dienoyl-CoA isomerase at 1.5 Å resolution reveals the importance of aspartate and glutamate sidechains for catalysis, *Structure 6*, 957−970.
32. Woods, A. S., and Ferre, S. (2005) Amazing stability of the arginine-phosphate electrostatic interaction, *J. Proteome Res. 4*, 1397−1402.
33. Mitchell, J. B., Nandi, C. L., McDonald, I. K., Thornton, J. M., and Price, S. L. (1994) Amino/aromatic interactions in proteins: is the evidence stacked against hydrogen bonding?, *J. Mol. Biol. 239*, 315−331.
34. Ehmann, D. E., Trauger, J. W., Stachelhaus, T., and Walsh, C. T. (2000) Aminoacyl-SNACs as small-molecule substrates for the condensation domains of nonribosomal peptide synthetases, *Chem. Biol. 7*, 765−772.
35. Otwinowski, Z., and Minor, W. (1997) Processing of X-ray Diffraction Data Collected in Oscillation Mode, in *Methods in Enzymology: Macromolecular Crystallography* (Carter, C. W., and Sweet, R. M., Eds.) Part A, pp 307−326, Academic Press, New York.
36. Brunger, A. T., Adams, P. D., Clore, G. M., DeLano, W. L., Gros, P., Grosse-Kunstleve, R. W., Jiang, J. S., Kuszewski, J., Nilges, M., Pannu, N. S., Read, R. J., Rice, L. M., Simonson, T., and Warren, G. L. (1998) Crystallography & NMR system: A new software suite for macromolecular structure determination, *Acta Crystallogr., D: Biol. Crystallogr. 54*, 905−921.
37. Tian, J., Sinskey, A. J., and Stubbe, J. (2005) Class III polyhydroxybutyrate synthase: involvement in chain termination and reinitiation, *Biochemistry 44*, 8369−8377.
38. Oguro, S., Akashi, T., Ayabe, S., Noguchi, H., and Abe, I. (2004) Probing biosynthesis of plant polyketides with synthetic *N*-acetylcysteamine thioesters, *Biochem. Biophys. Res. Commun. 325*, 561−567.
39. Jacobsen, J. R., Hutchinson, C. R., Cane, D. E., and Khosla, C. (1997) Precursor-directed biosynthesis of erythromycin analogs by an engineered polyketide synthase, *Science 277*, 367−369.
40. Bell, A. F., Wu, J., Feng, Y., and Tonge, P. J. (2001) Involvement of glycine 141 in substrate activation by enoyl-CoA hydratase, *Biochemistry 40*, 1725−1733.
41. D'Ordine, R. L., Bahnson, B. J., Tonge, P. J., and Anderson, V. E. (1994) Enoyl-coenzyme A hydratase-catalyzed exchange of the alpha-protons of coenzyme A thiol esters: a model for an enolized intermediate in the enzyme-catalyzed elimination?, *Biochemistry 33*, 14733−14742.
42. Hofstein, H. A., Feng, Y., Anderson, V. E., and Tonge, P. J. (1999) Role of glutamate 144 and glutamate 164 in the catalytic mechanism of enoyl-CoA hydratase, *Biochemistry 38*, 9508−9516.
43. Roth, J. P., Wincek, R., Nodet, G., Edmondson, D. E., McIntire, W. S., and Klinman, J. P. (2004) Oxygen isotope effects on electron transfer to O_2 probed using chemically modified flavins bound to glucose oxidase, *J. Am. Chem. Soc. 126*, 15120−15131.
44. Mattevi, A. (2006) To be or not to be an oxidase: challenging the oxygen reactivity of flavoenzymes, *Trends Biochem. Sci. 31*, 276−283.

BI701148B